

**SUPPLEMENTARY MATERIALS: NEURONAL RESILIENCE AND  
CALCIUM SIGNALING PATHWAYS IN THE CONTEXT OF  
SYNAPSE LOSS AND CALCIUM LEAKS: A COMPUTATIONAL  
MODELLING STUDY AND IMPLICATIONS FOR ALZHEIMER'S  
DISEASE\***

PIYUSH BOROLE<sup>†</sup>, JAMES M. ROSADO<sup>‡</sup>, MEIROSE NEAL<sup>‡</sup>, AND GILLIAN QUEISSER<sup>‡</sup>

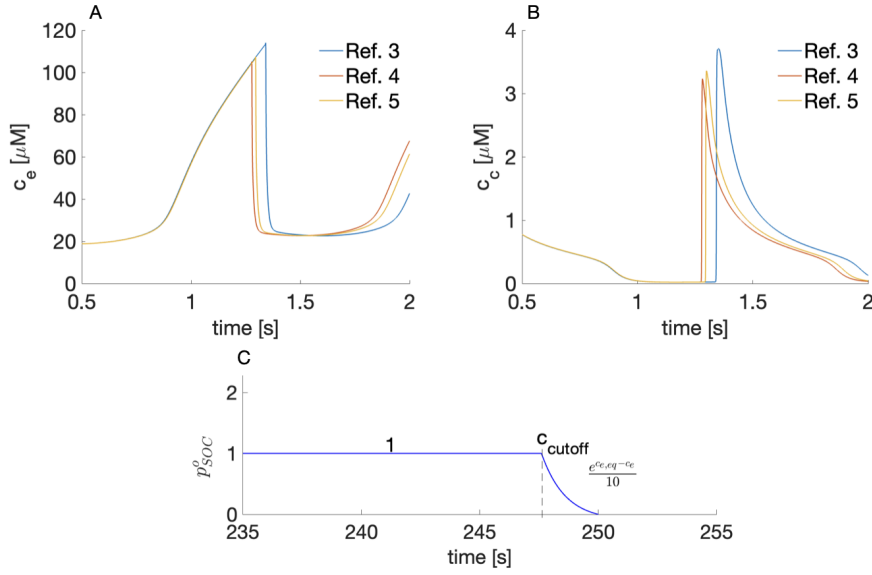


FIG. SM1. *Convergence analysis using different refinement levels. (A-B) concentration profiles for  $\text{Ca}^{2+}$  in the cytosol and ER, respectively on an unbranched neurite. The refinement levels were  $m = 1, 2, 3, 4, 5$ , with the edge length of  $\Delta x = 2.0, 1.0, 0.5, 0.25, 0.125 \mu\text{m}$  and time step  $\Delta t = 160, 80, 40, 20, 10 \text{ ms}$ , respectively. (C) open state probability of SOC ( $p_{SOC}^o$ ) is modeled after eq. ???. The value of  $p_{SOC}^o$  is set to 1 until it reaches a cutoff value ( $247.602 \mu\text{M}$ , calculated) after which it decays exponentially to zero.*

\*Submitted to the editors August 12, 2025

<sup>†</sup>University of Edinburgh, Edinburgh, Scotland, United Kingdom

<sup>‡</sup>Department of Mathematics, Temple University, Philadelphia, Pennsylvania, U.S.A.

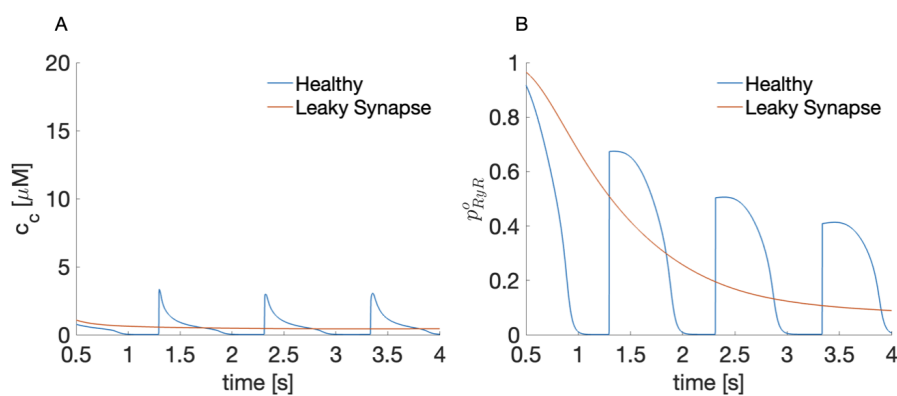


FIG. SM2. *RyR open state probability in healthy vs. leaky synapse in an unbranched neurite with 5Hz stimulation. (A) The  $\text{Ca}^{2+}$  profile at the soma in the healthy state causes 1Hz wave responses, where  $c_c$  is low during equilibrium. In leaky synapses, baseline  $c_c$  is elevated and no such wave response is observed. (B) The decrease of  $c_c$  levels to baseline in the healthy state allows  $p_{RyR}^o$  to also return to 0 after a wave event. However, in case of leaky synapses, the elevated  $c_c$  levels prevent  $p_{RyR}^o$  to return to 0 rapidly and thus hinders wave initiation.*

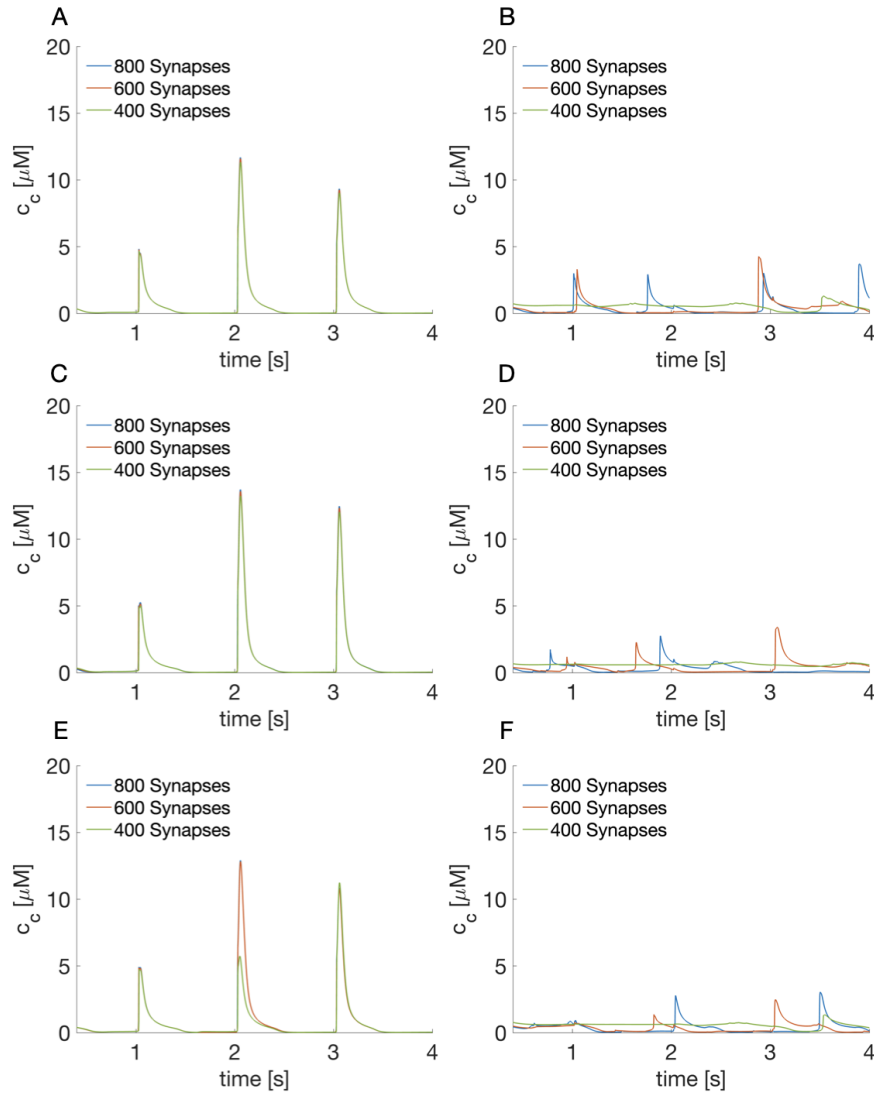


FIG. SM3. Comparing different electro-calcium coupling. (A-B) no VDCCs, i.e., no electrical coupling at 1Hz (A) and 5Hz (B) stimulation frequency. (C-D) N-Type VDCC coupling at 1Hz and 5Hz. This figure is intended to illustrate that coupling the calcium dynamics to the electrical signal is relevant and different results are to be expected when excluding electro-calcium coupling or including different types of VDCC.

TABLE SM1  
Model Parameters

| Parameter                                  | Symbol          | Value   | Reference  |
|--|-----------------|---|--|
| <i>Initial and equilibrium values</i>      |                 |   |  |
| Cytosolic $\text{Ca}^{2+}$                 | $c_c$           | 50 nM   | [SM4]  |
| ER $\text{Ca}^{2+}$                        | $c_e$           | 250 $\mu\text{M}$   | [SM4]  |
| Reference ER $\text{Ca}^{2+}$              | $c_e^{ref}$     | 250 $\mu\text{M}$   | [SM4]  |
| Extracellular $\text{Ca}^{2+}$             | $c_o$           | 1 mM  | [SM4]  |
| Total Calbindin D <sub>28k</sub> (Cytosol) | $b^{tot}$       | 40 $\mu\text{M}$  | [SM19, SM4]                                      |
| Total Calreticulin (ER)                    | $b_e^{tot}$     | 3.6 mM  | [SM18]   |
| <i>Diffusion/reaction</i>                  |                 |   |  |
| Diffusion coefficient ( $c_c$ )            | $D_c$           | 220 $\mu\text{m}^2\text{s}^{-1}$                              | [SM1, SM4]                                       |
| Diffusion coefficient (CalB)               | $D_c$           | 20 $\mu\text{m}^2\text{s}^{-1}$                               | [SM24, SM4]                                      |
| CalB forward rate                          | $\kappa_b^+$    | 27 $\mu\text{M}^{-1}\text{s}^{-1}$                            | [SM19, SM4]                                      |
| CalB backward rate                         | $\kappa_b^-$    | 19 $\text{s}^{-1}$  | [SM19, SM4]                                      |
| Diffusion coefficient ( $c_e$ )            | $D_{ce}$        | 10 $\mu\text{m}^2\text{s}^{-1}$                               | [SM6, SM17]                                      |
| Diffusion coefficient (CalR)               | $D_{be}$        | 27 $\mu\text{m}^2\text{s}^{-1}$                               | [SM18]   |
| CalR forward rate                          | $\kappa_{be}^+$ | 10 <sup>5</sup> $\text{M}^{-1}\text{s}^{-1}$                  | [SM18]   |
| CalR backward rate                         | $\kappa_{be}^-$ | 200 $\text{s}^{-1}$   | Calculated using<br>$K_d = 2 \text{ mM}$ ([SM2]) |
| <i>RyR channel</i>                         |                 |   |  |
| $o_1 \rightarrow c_1$                      | $k_a^-$         | 28.8 $\text{s}^{-1}$  | [SM14]   |
| $c_1 \rightarrow o_1$                      | $k_d^-$         | 1500 $\mu\text{M}^{-4}\text{s}^{-1}$                          | [SM14]   |
| $o_2 \rightarrow o_1$                      | $k_b^-$         | 385.9 $\text{s}^{-1}$   | [SM14]   |
| $o_1 \rightarrow o_2$                      | $k_b^+$         | 1500 $\mu\text{M}^{-3}\text{s}^{-1}$                          | [SM14]   |
| $c_2 \rightarrow o_1$                      | $k_c^-$         | 0.1 $\text{s}^{-1}$   | [SM14]   |
| $o_1 \rightarrow c_2$                      | $k_c^+$         | 1.75 $\text{s}^{-1}$  | [SM14]   |
| Reference current                          | $I_{RyR}^{ref}$ | $3.5 \times 10^{-18} \text{ mol s}^{-1}$                      | [SM26]   |
| <i>SERCA pumps</i>                         |                 |   |  |
| SERCA current                              | $I_S$           | $6.5 \times 10^{-21} \text{ mol } \mu\text{M} \text{ s}^{-1}$ | [SM5, SM4](Adapt.)                               |
|  | $K_S$           | 180 nM  | [SM25]   |
| SERCA density                              | $\rho_S$        | 2390 $\mu\text{m}^{-2}$                                       | [SM18](Approx.)                                  |
| <i>PMCA pumps</i>                          |                 |   |  |
| PMCA current                               | $I_P$           | $1.7 \times 10^{-23} \text{ mol s}^{-1}$                      | [SM10]   |
| Measure of $\text{Ca}^{2+}$ affinity       | $K_P$           | 60 nM   | [SM8]  |
| PMCA density                               | $\rho_P$        | 500 $\mu\text{m}^{-2}$  | [SM4](Estim.)                                    |
| <i>NCX pumps</i>                           |                 |   |  |
| NCX current                                | $I_N$           | $2.5 \times 10^{-21} \text{ mol s}^{-1}$                      | [SM10](adapt.)                                   |
| Measure of $\text{Ca}^{2+}$ affinity       | $K_N$           | 1.8 $\mu\text{M}$   | [SM10]   |
| NCX density                                | $\rho_N$        | 15 $\mu\text{m}^{-2}$   | [SM4](Estim.)                                    |
| <i>Store Operated Channels</i>             |                 |   |  |
| Single SOC current                         | $I_{SOC}^{ref}$ | 2.1 fA  | [SM9, SM13]                                      |
| Faraday's Constant                         | $F$             | 96485 C/mol   |  |
| Valency of $\text{Ca}^{2+}$ ion            | $z$             | 2   |  |
| Density of SOC                             | $\rho_{SOC}$    | 0.4 $\mu\text{m}^{-2}$  | choosen  |
| <i>A<math>\beta</math> pores</i>           |                 |   |  |
| Rate constant                              | $k_\beta$       | 1 $\text{s}^{-1}$   | [SM16, SM7]                                      |
| Cooperative factor                         | $m$             | 4   | [SM16, SM7]                                      |
| Concentration of A $\beta$                 | $a$             | 5 nM, 100 $\mu\text{M}$                                       | [SM7, SM20]                                      |
| <i>Miscellaneous</i>                       |                 |   |  |
| Input synaptic flux                        | $j_{syn}$       | $1 \times 10^{-6}$  | [SM4, SM23]                                      |

TABLE SM2  
*Model Parameters for VDCCs and electrical dynamics equations*

| Parameter   | Symbol                     | Value                          | Reference    |
|---|----------------------------|--------------------------------|--------------|
| <i>Voltage Dependent Calcium Channels (VDCC) N-type</i> |                            |                                |              |
| Valence   | $z_k, z_l$                 | 2, 1                           | [SM11, SM3]  |
| Voltage   | $V_{1/2,k}, V_{1/2,l}$     | -21 mV, -40 mV                 | [SM11, SM3]  |
| Rate parameter  | $\gamma_k, \gamma_l$       | 0, 0                           | [SM11, SM3]  |
| Rate parameter  | $K_k, K_l$                 | 1.7 ms, 70 ms                  | [SM11, SM3]  |
| Time constant   | $\tau_{0,k}, \tau_{0,l}$   | 1.7 ms, 70 ms                  | [SM11, SM3]  |
| Permeability of $\text{Ca}^{2+}$                        | $\bar{p}_{\text{Ca}^{2+}}$ | 3.8 $\text{cm}^3/\text{s}$     | [SM11, SM3]  |
| Faraday Constant  | $F$                        | 96485 C/mol                    | [SM11, SM3]  |
| Gas Constant  | $R$                        | 8.314 J/Kmol                   | [SM11, SM3]  |
| Temperature   | $T$                        | 310 Kelvin                     | [SM11, SM3]  |
| <i>Voltage Dependent Calcium Channels (VDCC) T-type</i> |                            |                                |              |
| Valence   | $z_k, z_l$                 | 2, 1                           | [SM3]        |
| Voltage   | $V_{1/2,k}, V_{1/2,l}$     | -36 mV, -68 mV                 | [SM3]        |
| Rate parameter  | $\gamma_k, \gamma_l$       | 0, 0                           | [SM3]        |
| Rate parameter  | $K_k, K_l$                 | 1.5 ms, 10 ms                  | [SM3]        |
| Time constant   | $\tau_{0,k}, \tau_{0,l}$   | 1.5 ms, 10 ms                  | [SM3]        |
| Permeability of $\text{Ca}^{2+}$                        | $\bar{p}_{\text{Ca}^{2+}}$ | 1.9 $\text{cm}^3/\text{s}$     | [SM11, SM3]  |
| <i>Parameters for Electrical Dynamics</i>               |                            |                                |              |
| Axonal Resistance                                       | $R_{ax}$                   | 0.75 $\Omega \cdot m$          | [SM21]       |
| Membrane Capacitance                                    | $C$                        | 0.01 F/ $m^2$                  | [SM21]       |
| $\text{K}^+$ Conductance                                | $\bar{g}_K$                | 50 S/ $m^2$                    | [SM21]       |
| $\text{Na}^{2+}$ Conductance                            | $\bar{g}_{Na}$             | 500 S/ $m^2$                   | [SM21]       |
| Leak Conductance  | $\bar{g}_l$                | 0.05 S/ $m^2$                  | [SM21]       |
| $\text{K}^+$ Reversal Potential                         | $V_K$                      | -0.90 V                        | [SM21]       |
| $\text{Na}^{2+}$ Reversal Potential                     | $V_{Na}$                   | 0.50 V                         | [SM21]       |
| Leak Reversal Potential                                 | $V_l$                      | -0.60 V                        | [SM21]       |
| $\text{Ca}^{2+}$ Reversal Potential                     | $V_{Ca}$                   | A function of $\text{Ca}^{2+}$ | [SM22, SM15] |
| Initial $\text{K}^+$ Channel Probability                | $n_0$                      | 0.00654                        | [SM12]       |
| Initial $\text{Na}^{2+}$ Channel Probability            | $m_0$                      | 0.00654                        | [SM12]       |
| Initial $\text{Na}^{2+}$ Channel Probability            | $h_0$                      | 0.9997                         | [SM12]       |
| Initial $\text{Ca}^{2+}$ Channel Probability            | $\sigma_0$                 | 0.9750                         | [SM22, SM15] |
| Calcium Current Parameter                               | $K$                        | 0.01 mol/ $m^3$                | [SM22, SM15] |

**SM1. Derivation for 1D reduced model.** In this section, we derive the 1D reduced PDEs for cytosolic  $\text{Ca}^{2+}$  concentration  $c_c$ . Fig. SM4 illustrates a section of unbranched neurite of width  $dx$ . The ER radius and the dendrite radius are denoted by  $r$  and  $R$  respectively. The fluxes ( $J_{PM}$ ) between cytosolic ( $\Omega_C$ ) and extracellular domain are on boundary  $\Gamma_{PM}$  while the fluxes ( $J_{ERM}$ ) between ER ( $\Omega_{ER}$ ) and cytosolic domains are on boundary  $\Gamma_{ERM}$ . At a given point, surface area of  $\Gamma_{PM} = 2\pi R$  and  $\Gamma_{ERM} = 2\pi r$ . The area of  $\Omega_C = \pi(R^2 - r^2)$  and  $\Omega_{ER} = \pi r^2$ .

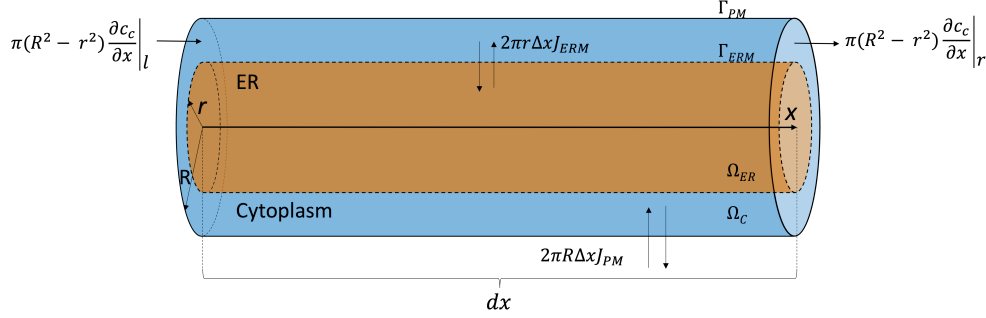


FIG. SM4. Illustration of a section of an unbranched neurite of width  $dx$  displaying mechanisms affecting cytosolic  $\text{Ca}^{2+}$  concentration.

We begin with the flux balance equation where each flux is scaled by the corresponding area/volume:

$$\begin{aligned} \pi(R^2 - r^2)\Delta x \frac{\partial c_c}{\partial t} &= \left( \pi(R^2 - r^2) \frac{\partial c_c}{\partial x} \Big|_r - \pi(R^2 - r^2) \frac{\partial c_c}{\partial x} \Big|_l \right) + 2\pi r \Delta x J_{ERM} \\ &\quad + 2\pi R \Delta x J_{PM} + \pi(R^2 - r^2)(k_b^-(b^{tot} - b) - k_b^+ b c_c) \\ (R^2 - r^2) \frac{\partial c_c}{\partial t} &= \frac{((R^2 - r^2) \frac{\partial c_c}{\partial x} \Big|_r - (R^2 - r^2) \frac{\partial c_c}{\partial x} \Big|_l)}{\Delta x} \\ &\quad + (R^2 - r^2)(k_b^-(b^{tot} - b) - k_b^+ b c_c) + 2r J_{ERM} + 2R J_{PM} \end{aligned}$$

Dividing by  $\Delta x$  and taking  $\Delta x$  to 0 leads to:

$$\begin{aligned} (R^2 - r^2) \frac{\partial c_c}{\partial t} &= \frac{\partial}{\partial x} \left( (R^2 - r^2) \frac{\partial c_c}{\partial x} \right) + (R^2 - r^2)(k_b^-(b^{tot} - b) - k_b^+ b c_c) \\ &\quad + 2r J_{ERM} + 2R J_{PM} \\ \frac{\partial c_c}{\partial t} &= \frac{1}{(R^2 - r^2)} \frac{\partial}{\partial x} \left( (R^2 - r^2) \frac{\partial c_c}{\partial x} \right) + (k_b^-(b^{tot} - b) - k_b^+ b c_c) \\ &\quad + \frac{2r}{R^2 - r^2} J_{ERM} + \frac{2R}{R^2 - r^2} J_{PM}, \quad \text{in } \Omega_C \end{aligned}$$

Equivalently, we derive the 1D reduced equations for  $c_e$ ,  $b$  and  $b_e$ :

$$\begin{aligned}
\frac{\partial c_e}{\partial t} &= \frac{1}{r^2} \frac{\partial}{\partial x} \left( r^2 D_c \frac{\partial c_e}{\partial x} \right) + (k_{be}^- (b_e^{tot} - b_e) - k_{be}^+ b_e c_e) \\
&\quad - \frac{2}{r} J_{ERM} + \frac{2}{r} J_{SOC}, \quad \text{in } \Omega_{ER} \\
\frac{\partial b}{\partial t} &= \frac{1}{(R^2 - r^2)} \frac{\partial}{\partial x} \left( (R^2 - r^2) D_b \frac{\partial b}{\partial x} \right) + (k_b^- (b^{tot} - b) - k_b^+ b c_c), \quad \text{in } \Omega_C \\
\frac{\partial b_e}{\partial t} &= \frac{1}{r^2} \frac{\partial}{\partial x} \left( r^2 D_{be} \frac{\partial b_e}{\partial x} \right) + (k_{be}^- (b_e^{tot} - b_e) - k_{be}^+ b_e c_e) \quad \text{in } \Omega_{ER}
\end{aligned}$$

## REFERENCES

- [SM1] N. L. ALLBRITTON, T. MEYER, AND L. STRYER, *Range of messenger action of calcium ion and inositol 1, 4, 5-trisphosphate*, Science, 258 (1992), pp. 1812–1815.
- [SM2] S. BAKSH AND M. MICHALAK, *Expression of calreticulin in escherichia coli and identification of its  $ca^{2+}$  binding domains.*, Journal of Biological Chemistry, 266 (1991), pp. 21458–21465.
- [SM3] L. J. BORG-GRAHAM, *Interpretations of Data and Mechanisms for Hippocampal Pyramidal Cell Models*, Springer US, Boston, MA, 1999, pp. 19–138, [https://doi.org/10.1007/978-1-4615-4903-1\\_2](https://doi.org/10.1007/978-1-4615-4903-1_2), [https://doi.org/10.1007/978-1-4615-4903-1\\_2](https://doi.org/10.1007/978-1-4615-4903-1_2).
- [SM4] M. BREIT AND G. QUEISSER, *What is required for neuronal calcium waves? a numerical parameter study*, The Journal of Mathematical Neuroscience, 8 (2018), <https://doi.org/10.1186/s13408-018-0064-x>, <https://doi.org/10.1186/s13408-018-0064-x>.
- [SM5] V. C. CHIU AND D. H. HAYNES, *Rapid kinetic studies of active  $ca^{2+}$  transport in sarcoplasmic reticulum*, The Journal of membrane biology, 56 (1980), pp. 219–239.
- [SM6] M. J. DAYEL, E. F. HOM, AND A. S. VERKMAN, *Diffusion of green fluorescent protein in the aqueous-phase lumen of endoplasmic reticulum*, Biophysical journal, 76 (1999), pp. 2843–2851.
- [SM7] J. DE CALUWÉ AND G. DUPONT, *The progression towards alzheimer's disease described as a bistable switch arising from the positive loop between amyloids and  $ca^{2+}$* , Journal of theoretical biology, 331 (2013), pp. 12–18.
- [SM8] N. L. ELWESS, A. G. FILOTEO, A. ENYEDI, AND J. T. PENNISTON, *Plasma membrane  $ca^{2+}$  pump isoforms 2a and 2b are unusually responsive to calmodulin and  $ca^{2+}$* , Journal of Biological Chemistry, 272 (1997), pp. 17981–17986.
- [SM9] D. GIL, A. H. GUSE, AND G. DUPONT, *Three-dimensional model of sub-plasmalemmal  $ca^{2+}$  microdomains evoked by the interplay between orai1 and insp3 receptors*, Frontiers in immunology, 12 (2021).
- [SM10] M. GRAUPNER, *A theory of plasma membrane calcium pump function and its consequences for presynaptic calcium dynamics*, Dissertation and Theses, (2003).
- [SM11] S. GREIN, M. STEPNIIEWSKI, S. REITER, M. M. KNODEL, AND G. QUEISSER, *1d-3d hybrid modeling-from multi-compartment models to full resolution models in space and time*, Frontiers in Neuroinformatics, 8 (2014), <https://doi.org/10.3389/fninf.2014.00068>, <https://doi.org/10.3389/fninf.2014.00068>.
- [SM12] A. L. HODGKIN AND A. F. HUXLEY, *A quantitative description of membrane current and its application to conduction and excitation in nerve*, The Journal of Physiology, 117 (1952), pp. 500–544, <https://doi.org/10.1113/jphysiol.1952.sp004764>, <https://doi.org/10.1113/jphysiol.1952.sp004764>.
- [SM13] M. HOTH AND R. PENNER, *Depletion of intracellular calcium stores activates a calcium current in mast cells*, Nature, 355 (1992), pp. 353–356.
- [SM14] J. KEIZER AND L. LEVINE, *Ryanodine receptor adaptation and  $ca^{2+}$  induced  $ca^{2+}$  release-dependent  $ca^{2+}$  oscillations*, Biophysical Journal, 71 (1996), pp. 3477–3487, [https://doi.org/10.1016/s0006-3495\(96\)79543-7](https://doi.org/10.1016/s0006-3495(96)79543-7), [https://doi.org/10.1016/s0006-3495\(96\)79543-7](https://doi.org/10.1016/s0006-3495(96)79543-7).
- [SM15] C. KOCH AND I. SEGEV, *Methods in Neuronal Modeling: From Synapses to Networks*, A Bradford book, MIT Press, 1989, <https://books.google.com/books?id=INvIQwAACAAJ>.
- [SM16] J. LATULIPPE, D. LOTITO, AND D. MURBY, *A mathematical model for the effects of amyloid beta on intracellular calcium*, PloS one, 13 (2018), p. e0202503.

- [SM17] E. McIVOR, S. COOMBES, AND R. THUL, *Three-dimensional spatio-temporal modelling of store operated  $ca2+$  entry: Insights into er refilling and the spatial signature of  $ca2+$  signals*, Cell calcium, 73 (2018), pp. 11–24.
- [SM18] S. MEANS, A. J. SMITH, J. SHEPHERD, J. SHADID, J. FOWLER, R. J. WOJCIKIEWICZ, T. MAZEL, G. D. SMITH, AND B. S. WILSON, *Reaction diffusion modeling of calcium dynamics with realistic er geometry*, Biophysical journal, 91 (2006), pp. 537–557.
- [SM19] A. MÜLLER, M. KUKLEY, P. STAUSBERG, H. BECK, W. MÜLLER, AND D. DIETRICH, *Endogenous  $ca2+$  buffer concentration and  $ca2+$  microdomains in hippocampal neurons*, Journal of Neuroscience, 25 (2005), pp. 558–565.
- [SM20] A. C. PAULA-LIMA, T. ADASME, C. SANMARTIN, A. SEBOLLELA, C. HETZ, M. A. CARRASCO, S. T. FERREIRA, AND C. HIDALGO, *Amyloid  $\beta$ -peptide oligomers stimulate ryr-mediated  $ca2+$  release inducing mitochondrial fragmentation in hippocampal neurons and prevent ryr-mediated dendritic spine remodeling produced by *bdnf**, Antioxidants & redox signaling, 14 (2011), pp. 1209–1223.
- [SM21] M. POSPISCHIL, M. TOLEDO-RODRIGUEZ, C. MONIER, Z. PIWKOWSKA, T. BAL, Y. FRÉGNAC, H. MARKRAM, AND A. DESTEXHE, *Minimal hodgkin-huxley type models for different classes of cortical and thalamic neurons*, Biological Cybernetics, 99 (2008), pp. 427–441, <https://doi.org/10.1007/s00422-008-0263-8>, <https://doi.org/10.1007/s00422-008-0263-8>.
- [SM22] A. PROTOPAPAS, M. VANIER, AND J. BOWER, *Simulating large networks of neurons*, in Methods in Neuronal Modeling: From Synapses to Networks, MIT Press, 01 1998, pp. 461–498.
- [SM23] J. M. ROSADO, *Ultrastructural neuronal modeling of calcium dynamics under transcranial magnetic stimulation*, 2022, <https://doi.org/10.34944/DSPACE/8010>, <https://scholarshare.temple.edu/handle/20.500.12613/8038>.
- [SM24] H. SCHMIDT, K. M. STIEFEL, P. RACAY, B. SCHWALLER, AND J. EILERS, *Mutational analysis of dendritic  $ca2+$  kinetics in rodent purkinje cells: role of parvalbumin and calbindin d28k*, The Journal of physiology, 551 (2003), pp. 13–32.
- [SM25] J. SNEYD, K. TSANEVA-ATANASOVA, J. BRUCE, S. STRAUB, D. GIOVANNUCCI, AND D. YULE, *A model of calcium waves in pancreatic and parotid acinar cells*, Biophysical Journal, 85 (2003), pp. 1392–1405, [https://doi.org/10.1016/s0006-3495\(03\)74572-x](https://doi.org/10.1016/s0006-3495(03)74572-x), [https://doi.org/10.1016/s0006-3495\(03\)74572-x](https://doi.org/10.1016/s0006-3495(03)74572-x).
- [SM26] A. TINKER, A. R. G. LINDSAY, AND A. J. WILLIAMS, *Cation conduction in the calcium release channel of the cardiac sarcoplasmic reticulum under physiological and pathophysiological conditions*, Cardiovascular Research, 27 (1993), pp. 1820–1825, <https://doi.org/10.1093/cvr/27.10.1820>, <https://doi.org/10.1093/cvr/27.10.1820>.